1999

Classification of Torbanite and Cannel Coal. II. Insights from Organic Geochemical and Multivariate Statistical Analysis

Zhiwen Han
Southern Illinois University Carbondale

Michael A. Kruge
Montclair State University, krugem@mail.montclair.edu

PREPRINT: Han Z. and Kruge M. A. (1999) Classification of torbanite and cannel coal. II. Insights from organic geochemical and multivariate statistical analysis. *International Journal of Coal Geology* **38**:203-218. https://doi.org/10.1016/S0166-5162(98)00014-7

Classification of torbanite and cannel coal. II. Insights from pyrolysis-GC/MS and multivariate statistical analysis.

Zhiwen Han[1] and Michael A. Kruge

Department of Geology, Southern Illinois University, Carbondale, IL 62901-4324 USA
[1]Present address: Deltech Engineering, 2893 E. La Palma Ave., Anaheim, CA 92806 USA

Abstract

Petrographic and megascopic criteria have traditionally been used as the basis for the classification of torbanite and cannel coal. For this study, it was hypothesized that modern analytical organic geochemical and multivariate statistical techniques could provide an alternative approach. Towards this end, the demineralized residues of 14 torbanite (rich in *Botryococcus*-related alginite) and cannel (essentially, rich in organic groundmass and/or sporinite) coal samples were analyzed by pyrolysis-gas chromatography/mass spectrometry (Py-GC/MS). Cluster analysis performed on the Py-GC/MS data clearly distinguished the torbanite from the cannel coal, demonstrating a consistency between the chemical properties and the petrographic composition. All the torbanite samples group into one cluster, their pyrolyzates having an overwhelming predominance of straight chain hydrocarbons, a characteristic typical of *Botryococcus*. The presence of the C_9-C_{26} *n*-α,ω-alkadiene series is the key feature distinguishing the torbanites from the other samples. The cannel coals exhibit more chemical diversity, reflecting their greater variability in petrographic composition. The Breckinridge cannel, dominated by a highly aliphatic lamalginitic groundmass, chemically fits the torbanite category. The bituminitic groundmass-dominated cannel coals fall into a cannel sub-cluster, their pyrolyzates having a characteristic predominance of *n*-alk-1-enes and *n*-alkanes (particularly the long-chain homologues), with no detectable alkadienes. The vitrinitic groundmass-dominated Ohio Linton cannel and the sporinite-rich Canadian Melville Island cannel are readily distinguishable from the other cannels by the relatively abundant aromatic and phenolic compounds in their pyrolyzates. The internal distribution patterns of alkylaromatic and alkylphenolic isomers are shown to be less significant in the classification of this sample set. Multivariate statistical analysis of the pyrolysis data not only successfully discriminated torbanites from cannel coals, but recognized subtler differences between the examples of these two coal types, in substantial agreement with the petrographic characterization. As such, these methods can substitute for or supplement the traditional microscope-based approach.

Keywords: torbanite, cannel coal, sapropelic coal, analytical pyrolysis-GC/MS, organic geochemistry

1. Introduction

Over the last two decades, analytical pyrolysis methods including pyrolysis-mass spectrometry (Py-MS), pyrolysis-gas chromatography (Py-GC) and pyrolysis-gas chromatography/mass spectrometry (Py-GC/MS) have been commonly used to characterize the chemical structure of solid organic matter in coals and petroleum source rocks (e.g., Larter, 1984; Meuzelaar et al., 1984; Nip et al., 1988; 1992; Hatcher et al., 1992; Hartgers et

al., 1994). In particular, recent studies have shown that detailed information about the macromolecular structure of the sedimentary organic matter can be obtained using Py-GC/MS (e.g., Hartgers et al., 1992; Sinninghe Damsté et al., 1988, 1993; Stankiewicz et al., 1994; 1996; Kruge et al., 1997).

Utilization of Py-GC/MS in a chemical structural study of torbanite can be traced back to late 1960's (Cane, 1969). Since then, use of various pyrolytic techniques to characterize torbanite as a natural algal concentrate has been reported (for instance: Largeau, 1980; Allan et al., 1980; Larter, 1984; Hower et al., 1986). A recent study compared alginite and groundmass density fractions from a Permian torbanite using Py-GC/MS (Han et al., 1995).

In this research, Py-GC/MS is used to characterize the torbanites and cannel coals in their entirety, as complex natural mixtures of various macerals and groundmass. These efforts will be focused on understanding the chemical characteristics of the bulk samples and the contributions of individual constituents. Petrographic and megascopic criteria have traditionally been used as the basis for the classification of torbanite and cannel coal. For this study, it was hypothesized that modern analytical organic chemical and multivariate statistical techniques would provide an alternative approach. This paper describes a test of this hypothesis, using a set of 14 torbanite and cannel coal samples of known petrographic composition (Han, 1995; Han et al., 1999).

2. Experimental methods

The provenance and petrographic data of the 14 torbanite and cannel samples used in this study are summarized in Table 1. They are from different locations in Australia, Canada, China, Scotland and the United States, ranging from Devonian to Permian in geological age, and of high volatile bituminous rank (Han et al., 1999).

The samples were crushed to less than 75 μm in size following standard procedures (ASTM, 1987) and then extracted with CH_2Cl_2 in a sonicator to remove the bitumen. The extraction residues were treated with 20% HCl for 24 hours and then with 30% HF for the same time period. Before pyrolysis, the samples underwent a second CH_2Cl_2 extraction to remove residual bitumen and any soluble organic contaminants introduced during demineralization.

The equipment used for flash Py-GC/MS was a CDS 120 Pyroprobe, connected to an HP 5890 gas chromatograph (GC) with an HP 5970 mass selective detector (MSD). The GC was equipped with a 25 m HP-1 column (0.2 mm i.d., film thickness 0.33 μm). The oven of the gas chromatograph was operated under the following program: isothermal for 5 min. at 0°C, temperature programmed at 5°/min. to 300°C, and then isothermal for 15 min. The MSD was operated in full scan mode (50-550 Da, 0.86 scans/sec., 70 eV ionization voltage). A measured amount of sample (≈1.0 mg), contained in a quartz tube placed in the center of a platinum coil, was pyrolyzed at 610°C in a flow of helium. The identification of the peaks was based on mass spectra, GC retention times, with reference to the U.S. National Bureau of Standards mass spectral library and the literature (Radke et al., 1990; Douglas et al., 1991; Hartgers et al., 1992; Nip et al., 1992; Sinninghe Damsté et al., 1989, 1992, 1993).

A total of 102 peaks representing the principal compounds in the pyrolyzates were quantitated using the ions specified (Table 2). These included *n*-alkadienes, *n*-alkenes, *n*-alkanes, alkylbenzenes, (alkyl)naphthalenes and (alkyl)phenols (Table 2). Although response factors were not applied, this relative quantitation was performed in a consistent manner for all samples and is therefore valid for the comparative purposes of this study. The peak areas were normalized to the maximum for each sample and then scaled by taking their square roots. The quantitation data set containing the 102 variables (i.e., the square roots of the

normalized peak areas) for each of the 14 samples were statistically processed using the SAS/STAT software package, Version 6 (SAS Institute Inc., 1990). Cluster analysis was performed using the average linkage method available in SAS/STAT.

3. Results and discussion

3.1. Summary of petrographic results

In hand specimen, the samples of both torbanite and cannel coal have a uniform, compact appearance, often with conchoidal fractures. Viewed under the microscope, they are composed of coarser maceral particles set in a fine-grained to amorphous groundmass (Han and Crelling, 1993). The macerals included *Botryococcus*-related alginite, sporinite, and detrital vitrinite and inertinite, plus minor amounts of resinite and cutinite. Based on composition, texture and fluorescence, the groundmass is further divided into three different types: lamalginitic, bituminitic and vitrinitic. A detailed discussion of the organic petrography of these samples has been presented (Han et al., 1999).

The distinction in petrographic composition between these torbanites and cannel coals is very clear. In the torbanite, *Botryococcus*-related alginite is the major constituent, whereas in the cannel coal, groundmass typically predominates and sporinite is normally abundant (Han et al., 1999). As summarized in Table 1, the torbanites display a gradual decrease in alginite content from sample 1 to sample 7. The Breckinridge cannel (sample 8) is characterized by a predominance of lamalginitic groundmass (79% by volume). Samples 10, 11, 12 and 13 are dominated by bituminitic groundmass, and also contain significant amounts of alginite (11-17%). The Linton cannel (sample 14) has a predominance of vitrinitic groundmass. The Canadian Melville Island cannel (sample 15) is particularly rich in sporinite.

3.2. Pyrolysis-gas chromatography/mass spectrometry

The principal compounds detected in the flash pyrolyzates of torbanite and cannel coals are the normal alkadienes, alkenes and alkanes, as well as (alkyl)benzenes, (alkyl)naphthalenes and (alkyl)phenols. These are readily seen on the total ion current traces (Figs. 1 to 4; also see Han, 1995). Alkylindenes, alkylthiophenes, and polycyclic aromatic compounds such as phenanthrene, anthracene, fluoranthene, chrysene, pyrene, and their alkylated derivatives are also usually detected as minor constituents. The compound distributions in the pyrolyzates are closely related to sample type.

The pyrograms of the seven torbanites have strong similarities. They show a predominance of the *n*-alk-1-ene and *n*-alkane homologous series (Fig. 1), consistent with previous reports (Cane, 1969; Largeau et al., 1980; Larter, 1984). In addition, a series of *n*-α,ω-alkadienes is detected, a characteristic feature of *Botryococcus*-related alginite pyrolyzates (e.g., Gatellier et al., 1993; Han et al., 1995). Relative concentrations of aromatic and phenolic compounds are very low.

In contrast, the compound distribution patterns of the cannel coal pyrolyzates vary widely from sample to sample. The pyrolyzate produced by the Breckinridge cannel (sample 8) shows a predominance of *n*-alkane/alkene pairs, with relatively low concentrations of aromatic and phenolic compounds. The C_9-C_{26} *n*-α,ω-alkadiene homologous series was detected as well. For the bituminitic groundmass-dominated cannel coals (samples 10-13), the distributions of pyrolysis products are basically similar to each other. They exhibit a strong predominance of the alkene/alkane pairs (e.g., sample 13, Fig. 2), especially the longer chain homologues (C_{18}-C_{28}), but lack detectable alkadienes. Aromatic and phenolic compounds are relatively more abundant than in the case of torbanite pyrolyzates (compare the expanded TIC traces in Fig. 1 and Fig. 2). In addition to the straight chain aliphatics, the

pyrolyzate of the Ohio Linton cannel (sample 14) has high relative concentrations of alkylbenzenes, alkylnaphthalenes and alkylphenols, clearly attributable to the dominant vitrinitic groundmass, which has been determined to be chemically similar to vitrinite (Han, 1995).

Fig. 4 shows the pyrolysis products of the Canadian Melville Island cannel, which is mostly composed of sporinite (75% by volume) and vitrinite. The pyrolyzate is characterized by a clear predominance of alkylbenzenes, alkylnaphthalenes and alkylphenols. Normal hydrocarbons up to C_{33} are also relatively abundant. Minor amounts of polycyclic aromatic hydrocarbons, such as phenanthrene, anthracene, fluoranthene, chrysene, pyrene, and their alkylated derivatives are present. Generally, the pyrolyzate shows a character intermediate between sporinite (Han, 1995) and vitrinite pyrolyzates (Nip et al., 1988; Hartgers et al., 1994; Kruge and Bensley, 1994).

3.3. Cluster analysis

Two major clusters are evident on the dendrogram summarizing the results of the multivariate statistical analysis of the pyrolysis data (Fig. 5). The first cluster includes all seven torbanite samples, plus the Breckinridge cannel (sample 8), which is dominated by a highly aliphatic lamalginitic groundmass (Han et al., 1999). The second cluster included all the other cannel coals and is in turn divided into two sub-clusters: A and B.

A comparison of Figure 5 with the petrographic data in Table 1 shows that clustering of the 14 torbanite and cannel coal samples based on chemical data essentially replicates the petrographic classification. In the torbanite cluster, samples 4 and 6 are the most closely related. Both of them are characterized by a predominance of alginite and bituminitic groundmass. They are in turn joined to Sample 7, which contains relatively less alginite but more bituminitic groundmass. The Indiana torbanite (sample 5) is closely correlated to the Breckinridge cannel (sample 8). Both their pyrolyzates showed a predominance of longer chain hydrocarbons (Han, 1995). The two alginite-dominated torbanites, samples 1 and 2, are also closely linked. The torbanite cluster is completed with the addition of another alginite-dominated sample, the South Africa torbanite (Sample 3).

Four of the cannel coals group in sub-cluster A. They are all characterized by a predominance of bituminitic groundmass, plus about 10% sporinite. Within this sub-cluster, samples 11, 12 and 13 show the closest affinities, while sample 10 is more distantly related. The remaining cannels (samples 14 and 15, the Linton and the Melville) are distinct from the rest but have some chemical similarities to each other, forming sub-cluster B.

3.4. Chemical significance of cluster analysis results

3.4.1. Pyrolyzate composition.

Fig. 6 presents the relative concentrations of the six main compound families present in the pyrolyzates: *n*-α,ω-alkadienes, *n*-alk-1-enes, *n*-alkanes, C_1-C_3 alkylbenzenes, C_0-C_2 (alkyl)naphthalenes and C_0-C_2 (alkyl)phenols. The eight samples in the torbanite cluster are distinguished from the cannel cluster by the presence of the alkadiene series. From top to bottom in Figure 6, the torbanite samples are arranged by decreasing relative concentration of alkadienes, while the cannel coals are arrayed by relative phenol concentration.

Samples in the torbanite cluster consistently possess a predominance of straight chain aliphatics (nearly 80% of the total). Alkylbenzenes, alkylnaphthalenes and alkylphenols account for only about 20%. As mentioned above, the presence of *n*-α,ω-alkadienes is a characteristic feature of (*Botryococcus*-related) alginite pyrolyzates. Hence the detection of the alkadienes in the torbanite pyrolyzates is obviously attributable to the presence of large amounts of alginite. A linear relationship exists between the relative alkadiene concentrations

and alginite content, with a correlation coefficient of 0.91 (Fig. 7). The Breckinridge cannel pyrolyzate (sample 8) chemically fits the torbanite cluster, having a predominance of aliphatics, including *n*-α,ω-alkadiene series, hallmarks of the lamalginitic groundmass (Han, 1995), which is its majority constituent. This sample was also shown to be different from the bituminitic groundmass-dominated cannels by its significantly higher Hydrogen Index (Han et al., 1999). Compared with other torbanite cluster members, the South African torbanite (sample 3) produced relatively less alkanes but more alkylbenzenes. Its groundmass fraction is shown to be dissimilar to other groundmass fractions, also by having more alkylbenzenes but less long chain hydrocarbons in the pyrolyzate (Han, 1995). Thus, sample 3 is different from the other torbanite cluster members (Fig. 5), likely due to the influence of its somewhat atypical groundmass.

No alkadienes were detected in the pyrolyzates of the cannel coals (e.g., Figs. 2-4), even though some of them contain a few percent alginite (Table 1). Pyrolyzates of samples 10, 11, 12 and 13 of sub-cluster A displayed a predominance of normal alkenes and alkanes. The relative concentrations of alkylbenzenes, alkylnaphthalenes and alkylphenols are only slightly higher than those of the torbanite. The highly aliphatic nature of the cannel coal pyrolyzates of sub-cluster A is clearly attributable to the predominance of bituminitic groundmass (about 60 to 70% by volume), the pyrolyzates of which are particularly enriched in straight chain aliphatics (Han, 1995).

The pyrolyzates of the remaining two samples (14 and 15) are distinctive due to the predominance of benzenes, naphthalenes and especially phenolic compounds (Figs. 3, 4 and 6). Compared to the other samples, the pyrolyzates of the Linton cannel (sample 14) and particularly the Melville Island cannel (sample 15) contains relatively less aliphatics (Fig. 6). Petrographically, sample 14 has a predominance of a vitrinitic groundmass (63% by volume), plus about 16% alginite and sporinite. The Melville Island cannel is comprised of 65% sporinite and 33% vitrinite. As reported by Han (1995), the pyrolyzates of the sporinite and vitrinite fractions from this cannel, contain about 40% and 20% normal hydrocarbons, respectively. Thus, the relatively low normal hydrocarbon concentration (about 30%) of the Melville Island cannel pyrolyzate reflects a composition intermediate between its constituent sporinite and vitrinite. Although the two samples of "sub-cluster B" have major petrographic differences, their chemical similarities (having macerals prone to the production of phenols and aromatic hydrocarbons upon pyrolysis) led to the recognition of a moderate level of affinity by the cluster analysis (Fig. 5).

3.4.2. Distribution of normal hydrocarbons

There is a marked difference in the average distribution of the total normal hydrocarbons (sum of alkadienes, alkenes and alkanes) of the torbanite cluster and cannel sub-cluster A pyrolyzates (Fig. 8). The torbanite pyrolyzates are characterized by a predominance of shorter chain aliphatics ($< C_{20}$), with a maximum at C_{10}, giving a C_{21}-C_{33}/C_8-C_{20} ratio of 0.38. Such a distribution pattern resembles that produced by alginite concentrates of the *Botryococcus* type (Han, 1995), further confirming that the alginite component is responsible for most of the aliphatics in torbanite pyrolyzates. However, there are some differences between the pyrolyzates of the torbanites and the alginite concentrates. For example, the slightly higher abundance of mid-length chains (C_{15}-C_{25}) in the torbanites could be explained as the effect of other constituents, especially the groundmass and vitrinite particles.

The average aliphatic distribution of cannel sub-cluster A pyrolyzates (Fig. 8B) is similar to that of the bituminitic groundmass concentrates (Han, 1995). The aliphatics show a broad maximum from C_{10}-C_{15}, as well as enrichment in the C_{16}-C_{26} range, which raises the C_{21}-C_{33}/C_8-C_{20} ratio up to 0.50, significantly higher than the torbanite value of 0.38. The

aliphatics of the Linton cannel pyrolyzate (Fig. 3) are relatively lower in concentration but generally similar in distribution to those of other cannel coals (Fig. 2). The aliphatics are relatively enriched in longer chains, with a C_{21}-C_{33}/C_8-C_{20} ratio of 0.54. The aliphatic distribution of the Melville Island cannel pyrolyzate is not clear from the TIC chromatogram (Fig. 4) due to the high concentrations of aromatic and phenolic compounds. But the ratio of C_{21}-C_{33}/C_8-C_{20} (0.35) indicated a predominance of short chain aliphatics, showing that the aliphatics were mainly generated by the sporinite (Han, 1995), which comprised 65% of this sample.

3.4.3. Alkylbenzene and alkylnaphthalene distributions

Multivariate statistical processing of the relative concentration data from the pyrolyzates reveals that alkylaromatic hydrocarbons with a single, linear side chain correlated positively with straight chain aliphatic hydrocarbons. This phenomenon can be observed directly on the pyrograms. Ethylbenzene (peak B2a) and *n*-propylbenzene (B3a) are relatively more important (compared to other alkylbenzenes) in the aliphatic-rich torbanite pyrolyzates than in those of other samples, as can be seen by careful comparison of Figures 1 and 3. Because of coelution problems, the behavior of *n*-propylbenzene can be observed more readily on m/z 91+105+120 mass chromatograms (Fig. 9). An analogous effect is seen among the C_2-alkylnaphthalenes. Ethylnaphthalene (N2a) distinctly shows a greater relative importance on the m/z 155+170 mass chromatogram of the Scottish torbanite pyrolyzate, compared to the vitrinitic Ohio cannel (Fig. 10).

We can speculate that the alkylaromatic hydrocarbons with linear side chains are enhanced due to aromatization during pyrolysis of the highly-aliphatic torbanites. Alternatively, these aromatic structures may have arisen due to burial alteration. In any event, they provide a further point to be used in the chemical classification of sapropelic coals. Except for these subtle features, the alkylbenzene and alkylnaphthalene isomer distributions do not exhibit great differences within the sample set. They are of lesser importance in the classification than are the relative concentrations of the various compound classes discussed above.

4. Conclusions

Cluster analysis of the Py-GC/MS data clearly distinguishes the torbanite from the cannel coal pyrolyzates, demonstrating the consistency between the chemical properties and the petrographic composition. All seven torbanite pyrolyzates group in one cluster, due to their similar, aliphatic nature. In contrast, the cannel coals are more diverse chemically, due to greater variability in petrographic composition. The Breckinridge cannel, dominated by an aliphatic lamalginitic groundmass, chemically fits the torbanite category. The bituminitic groundmass-dominated cannel coal pyrolyzates clearly grouped together. The vitrinitic groundmass-dominated Linton cannel and the sporinite-rich Melville Island cannel pyrolyzates showed some chemical similarities, due to a coincidental predominance of terrestrial organic matter.

Comparison of pyrolysis data for the whole coals with that of the individual macerals and groundmass types indicates that chemical properties of the whole coals are strongly related to the dominant petrographic constituents. The seven torbanite pyrolyzates are generally similar to those of alginite. They are distinguished by an overwhelming predominance of straight chain aliphatics, notably including the *n*-α,ω-alkadienes. The alkadienes are the key components which enabled the cluster analysis to distinguish torbanites from cannel coals.

The pyrolyzates of four cannel coals of sub-cluster A are very similar to those produced by the dominant bituminitic groundmass (60-70% by volume). They displayed a predominance of *n*-alk-1-enes and *n*-alkadienes, without detectable alkadienes. Their characteristically equable carbon number distributions of normal hydrocarbons are attributable to the influence of the bituminitic groundmass.

The Linton and Melville Island cannels are distinguished from other cannel coals and torbanites by the relatively abundant aromatic and phenolic compounds in their pyrolyzates. The high relative concentrations of such compounds in the Linton cannel are clearly due to the contribution of the dominant vitrinitic groundmass. The pyrolyzate of the Melville Island cannel is comparable to that of sporinite, its majority constituent maceral.

For this suite of torbanites and cannel coals, a small number of features of their pyrolyzates were shown to be sufficient for their correct classification by cluster analysis. The most important of these are the presence or absence of *n*-alkadienes and the summed relative concentrations of (alkyl)phenols and (alkyl)aromatic hydrocarbons. Using a simplified approach based on these insights, such coals (and oil-prone lacustrine kerogens by extension) could be recognized, evaluated and classified by geochemical means.

Acknowledgments

We gratefully acknowledge the contributions of samples by our colleagues, R.M.S. Falcon (Falcon Research Laboratory Ltd., South Africa), Fariborz Goodarzi (Geological Survey of Canada), James C. Hower, (Center for Applied, Energy Research, University of Kentucky), and Adrian Hutton (Department of Geology, University of Wollongong, Australia). We also wish to thank John C. Crelling, James Staub, John E. Utgaard, Harry Marsh, Russell Dutcher, David F. Bensley, Stephen Palmer, Bill Huggett, Corliss Thies and Artur Stankiewicz for their advice and technical assistance. The thoughtful comments of A. C. Cook and G. E. Michael helped to improve the final version of the manuscript.

References

Allan, J., Bjorøy, M., Douglas, A. G., 1980, A geochemical study of the exinite group maceral alginite, selected from three Permo-Carboniferous torbanites, in: Douglas, A. G., Maxwell, J. R. (Eds.), Advances in Organic Geochemistry 1979, Pergamon, Oxford, pp. 599-618.

American Society for Testing Materials (ASTM), 1987. Annual Book of ASTM Standards: Part 26: Gaseous Fuels; Coal and Coke; Atmospheric Analysis. ASTM, Philadelphia.

Cane, R. F., 1969. Coorongite and the genesis of oil shales. Geochim. Cosmochim. Acta 33, 257-265.

Douglas, A. G., Sinninghe Damsté, J. S., Fowler, M. G., Eglinton, T. I., de Leeuw, J. W., 1991. Unique distributions of hydrocarbons and sulphur compounds by flash pyrolysis from the fossilized alga *Gloeocapsomorpha prisca*, a major constituent in one of four Ordovician kerogens. Geochim. Cosmochim. Acta 55, 275-291.

Gatellier, J.-P. L. A., de Leeuw, J. W., Sinninghe Damsté, J. S., Derenne, S., Largeau, C., Metzger, P., 1993. A comparative study of macromolecular substances of a Coorongite and cell walls of the extant alga *Botryococcus braunii*. Geochim. Cosmochim. Acta 57, 2053-2068.

Han, Z., 1995. Organic geochemistry and petrology of torbanite, cannel coal and their constituent macerals. Ph.D. thesis, Southern Illinois University at Carbondale, 235 p.

Han, Z., Crelling, J. C., 1993. Observations on the petrographic composition of cannel and boghead coals. Proceeding of 7th International Conference on Coal Science, Banff, Alberta, Canada, Vol. I, 144-147.

Han, Z., Kruge, M. A., Crelling, J. C., Stankiewicz, B. A., 1995. Organic geochemical characterization of the density fractions from a Permian torbanite. Org. Geochem. 22, 39-50.

Han, Z., Kruge, M. A., Crelling, J. C., Bensley, D. F. Classification of torbanite and cannel coal. I. Insights from petrographic analysis of density fractions. Int. J. Coal Geol. 38, 181-202 (this issue).

Hartgers, W. A., Sinninghe Damsté, J. S., de Leeuw, J. W., 1992. Identification of C_2-C_4 alkylated benzenes in flash pyrolyzates of kerogens, coals and asphaltenes. J. Chrom. 606, 211-220.

Hartgers, W. A., Sinninghe Damsté, J. S., de Leeuw, J. W., Ling, Y., Dyrkacz, G. R., 1994. Molecular characterization of two Carboniferous coals and their constituting maceral fractions. Energy & Fuels 8, 1055-1067.

Hatcher, P. G., Faulon, J., Wenzel, K. A., Cody, G. D., 1992. A structural model for lignin-derived vitrinite from high-volatile bituminous coal (coalified wood). Energy & Fuels 6, 813-820.

Hower, J. C., Taulbee, D. N., Poole, C., Kuehn, D. W., 1986. Petrology and Geochemistry of the Breckinridge seam - A torbanite from Western Kentucky. 1986 Eastern Oil Shale Symp. Proc., pp. 267-280.

Kruge M. A., Landais P., Bensley D. F., Stankiewicz B. A., Elie M., Ruau O., 1997, Separation and artificial maturation of macerals from Type II kerogen. Energy & Fuels 11, 503-514.

Kruge M. A., Bensley D. F., 1994. Flash pyrolysis-gas chromatography-mass spectrometry of Lower Kittanning vitrinites. Changes in distributions of polyaromatic hydrocarbons as a function of coal rank, in: Mukhopadhyay P. K., Dow W. (Eds.), Vitrinite Reflectance as a Maturity Parameter, Amer. Chem. Soc. Symp. Series 570. pp. 136-148.

Largeau, C., Casadevall, E., Berkaloff, C., 1980. Sites of accumulation and composition of hydrocarbons in *Botryococcus braunii.* Phytochem. 19, 1043- 1051.

Larter, S. R., 1984. Application of analytical pyrolysis techniques to kerogen characterization and fossil fuel exploration/exploitation, in: Voorhees, K. E. (Ed.), Advances in Analytical Pyrolysis, Vol. II, Butterworths, London, pp. 212-272.

Meuzelaar, H. L. C., Harper, A. M., Pugmire, R. J., Karas, J., 1984. Characterization of coal maceral concentrates by Curie-point pyrolysis mass spectrometry. Int. J. Coal Geol. 4, 143-171.

Nip, M., de Leeuw, J. W., Schenck, P. A., 1988. The characterization of eight maceral concentrates by means of Curie point pyrolysis-gas chromatography and Curie point pyrolysis-gas chromatography-mass spectrometry. Geochim. Cosmochim. Acta 52, 637-648.

Nip, M., de Leeuw, J. W., Crelling, J. C., 1992. Chemical structure of bituminous coal and its constituent maceral fractions as revealed by flash pyrolysis. Energy & Fuels 6, 125-136.

Radke M., Garrigues P., Willsch H., 1990. Methylated dicyclic and tricyclic aromatic hydrocarbons in crude oils from the Handil field, Indonesia. Org. Geochem. 15, 17-34.

SAS Institute Inc., 1990. SAS/STAT software package, Version 6, 4th ed., SAS Institute Inc., Cary, North Carolina, U.S.A.

Sinninghe Damsté, J. S., Kock-van Dalen, A. C., de Leeuw, J. W., Schenck, P. A., 1988. Identification of homologous series of alkylated thiophenes, thiolanes, thianes and benzothiophenes present in pyrolyzates of sulfur-rich kerogens. J. Chrom. 435, 435-452.

Sinninghe Damsté, J. S., Eglinton, T. I., de Leeuw, J. W., Schenck, P. A., 1989. Organic sulphur in macromolecular sedimentary organic matter: I. Structure and origin of sulphur-containing moieties in kerogen, asphaltenes and coal as revealed by flash pyrolysis. Geochim. Cosmochim. Acta 53, 873-889.

Sinninghe Damsté, J. S., De Las Heras, F. X. C, de Leeuw, J. W., 1992. Molecular analysis of sulphur-rich brown coals by flash pyrolysis-gas chromatography- mass spectrometry. J. Chrom. 607, 361-376.

Sinninghe Damsté, J. S., de Las Heras, X. C., Van Bergen, P. F., de Leeuw, J. W., 1993. Characterization of Tertiary Catalan lacustrine oil shales: Discovery of extremely organic sulphur- rich Type I kerogens. Geochim. Cosmochim. Acta 57, 389-415.

Stankiewicz, B. A., Kruge, M. A., Crelling, J. C., Salmon, G. L., 1994, Density gradient centrifugation: Application to the separation of macerals of Type I, II, and III sedimentary organic matter. Energy & Fuels 8, 1523-1521.

Stankiewicz, B. A., Kruge, M. A., Mastalerz, M., Salmon, G. L., 1996, Geochemistry of the alginite and amorphous organic matter from Type II-S kerogens. Org. Geochem. 24, 495-509.

Table 1. Provenance and petrographic composition of the torbanite and cannel coal samples. Sample numbers are the same as those used by Han et al. (1999).

ID	SIU ID	Locations	Age	Type	Alg	Spor	C+R	Vitr	Inert	GM
1	2262	Alpha, Australia	Permian	Torbanite	89.00	0.50	nd	2.60	1.70	6.20
2	2331	Middle River, Australia	Permian	Torbanite	76.70	1.40	nd	4.20	3.90	13.80
3	668	Transvaal, South Africa	Permian	Torbanite	69.70	3.50	nd	1.60	4.00	21.30
4	670	Joadja, Australia	Permian	Torbanite	44.50	8.10	1.00	6.60	7.70	32.20
5	2248	Cannelburg, IN, USA	Westphalian	Torbanite	40.60	10.90	0.30	2.00	3.80	42.50
6	1210	Torbane, Scotland, UK	Westphalian	Torbanite	37.40	13.10	nd	2.10	7.80	39.70
7	2244	Shanxi, China	Permian	Torbanite	21.40	6.00	1.10	8.10	11.60	51.90
8	646	Breckinridge, KY, USA	Westphalian	Cannel	4.50	1.80	nd	12.40	2.10	79.20
10	892	KY, USA	Westphalian	Cannel	2.70	11.00	1.70	3.20	7.60	73.80
11	1319	Raleigh, WV, USA	Westphalian	Cannel	0.10	12.70	0.50	7.70	8.50	70.60
12	1827A	Kanawha, WV, USA	Westphalian	Cannel	0.30	11.10	0.20	11.20	10.10	67.20
13	1827B	Kanawha, WV, USA	Westphalian	Cannel	4.80	17.30	2.70	2.60	9.70	63.00
14	2123	Linton, OH, USA	Westphalian	Cannel	2.70	13.80	0.40	6.80	12.90	63.40
15	2067	Melville Island, Canada	Devonian	Cannel	0.00	64.90	nd	33.00	0.30	1.80

Table 2. Compounds and MS ions used in quantitation. Codes are used to identify peaks in Figs. 1-4, 9 and 10.

Code	Compounds	MS ions (m/z)
●	C_9–C_{26} alkadienes	55 + 57
○	C_8–C_{33} *n*-alk-1-enes	55 + 57
□	C_8–C_{33} *n*-alkanes	55 + 57
B1	Methylbenzene (toluene)	91 + 92
B2a	2-ethylbenzene	91 + 106
B2b	1,3- and 1,4-dimethylbenzenes	91 + 106
B2c	1,2-dimethylbenzene	91 + 106
B3a	propylbenzene	105 + 120
B3b	1-ethyl-3-methylbenzene	105 + 120
B3c	1-ethyl-4-methylbenzene	105 + 120
B3d	1,3,5-trimethylbenzene	105 + 120
B3e	1-ethyl-2-methylbenzene	105 + 120
B3f	1,2,4-dimethylbenzene	105 + 120
B3g	1,2,3-trimethylbenzene	105 + 120
N0	Naphthalene	128
N1a	2-methylnaphthalene	141 + 142
N1b	1-methylnaphthalene	141 + 142
N2a	2-ethylnaphthalene	141 + 156
N2b	2,6-dimethylnaphthalene	141 + 156
N2c	2,7-dimethylnaphthalene	141 + 156
N2d	1,3-dimethylnaphthalene	141 + 156
N2e	1,7- and 1,6-dimethylnaphthalenes	141 + 156
N2f	2,3-, 1,4- and 1,5-dimethylnaphthalenes	141 + 156
N2g	1,2-dimethylnaphthalene	141 + 156
F0	Phenol	94
F1a	2-methylphenol	107 + 108
F1b	4 and 3-methylphenols	107 + 108
F2a	2,6-dimethylphenol	107 + 122
F2b	2-ethylphenol	107 + 122
F2c	2,4-dimethylphenol	107 + 122
F2d	2,5-dimethylphenol	107 + 122
F2e	4-ethylphenol	107 + 122
F2f	3-ethylphenol and 3,5-dimethylphenol	107 + 122
F2g	2,3-dimethylphenol	107 + 122
F2h	3,4-dimethylphenol	107 + 122

Fig. 1. Total ion current (TIC) chromatogram of the flash pyrolyzates of the Scottish torbanite (sample 6, alginite-dominated). Part of the chromatogram is enlarged to show detail. Numbers below chromatograms are *n*-alkane carbon numbers. See Table 2 for peak identification.

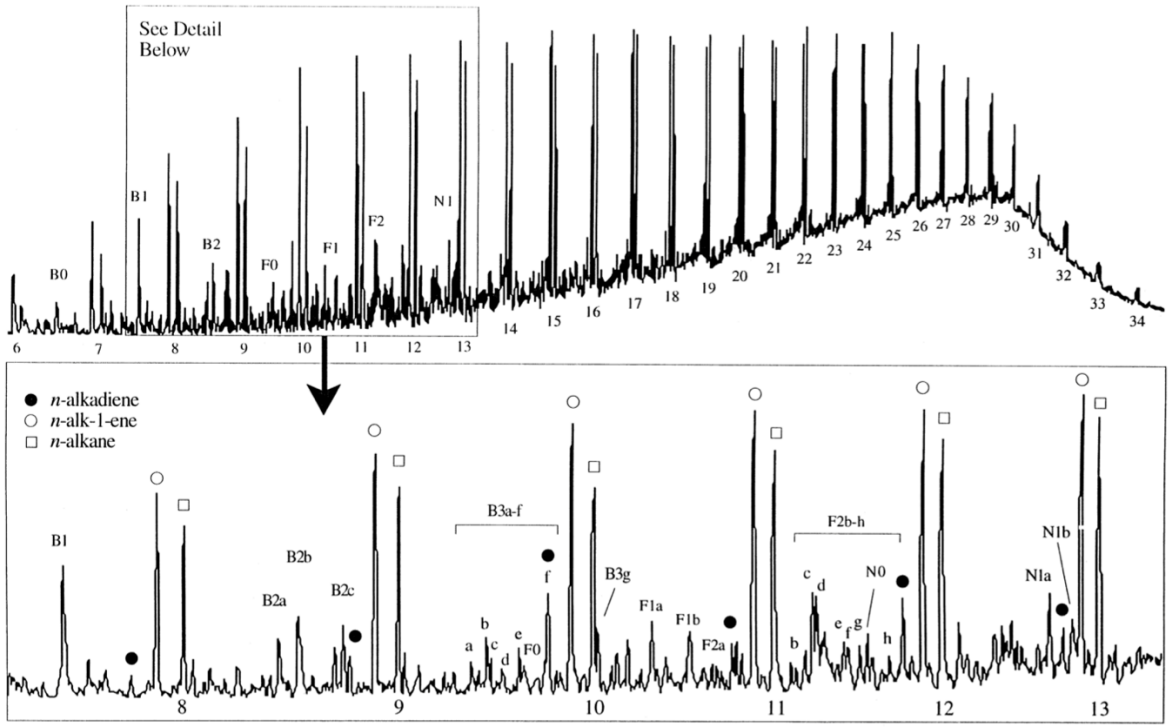

Fig. 2. Total ion current (TIC) chromatogram of the flash pyrolyzates of the Kanawha cannel coal of West Virginia, USA (sample 13, bituminitic groundmass-dominated). Part of the chromatogram is enlarged to show detail. Numbers below chromatograms are *n*-alkane carbon numbers. See Table 2 for peak identification.

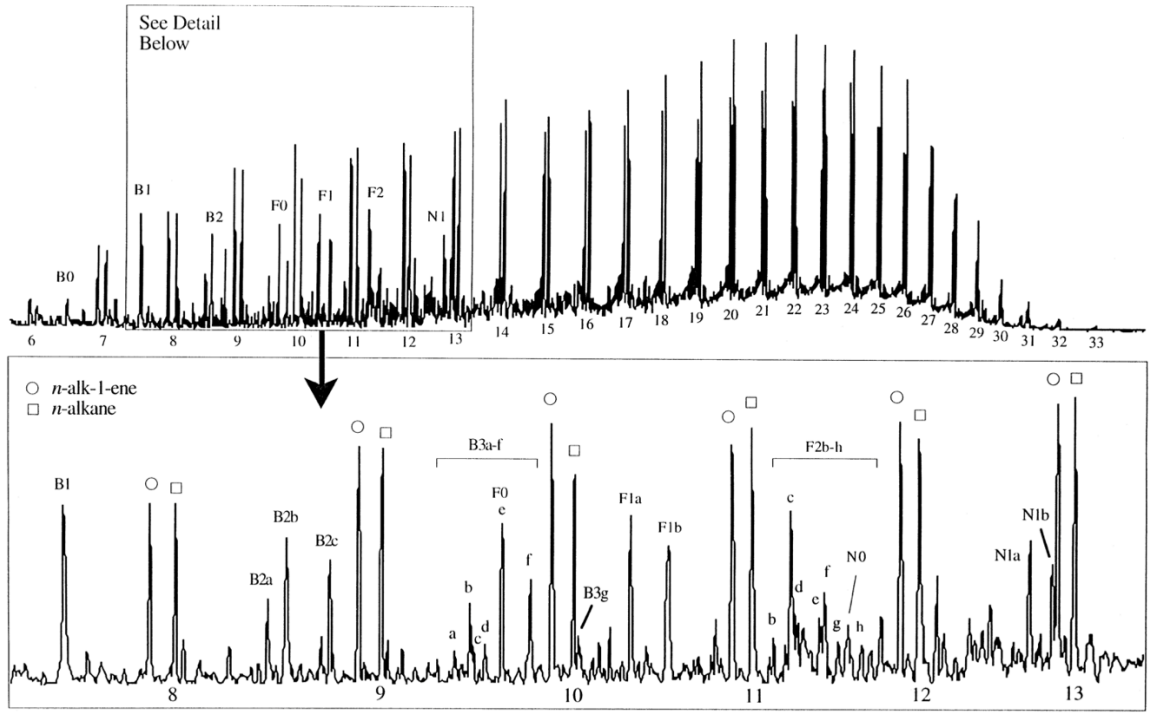

Fig. 3. Total ion current chromatogram (TIC) of the flash pyrolyzates of the Linton cannel coal of Ohio, USA (sample 14, vitrinitic groundmass-dominated). Part of the chromatogram is enlarged to show detail. Numbers below chromatograms are *n*-alkane carbon numbers. See Table 2 for peak identification.

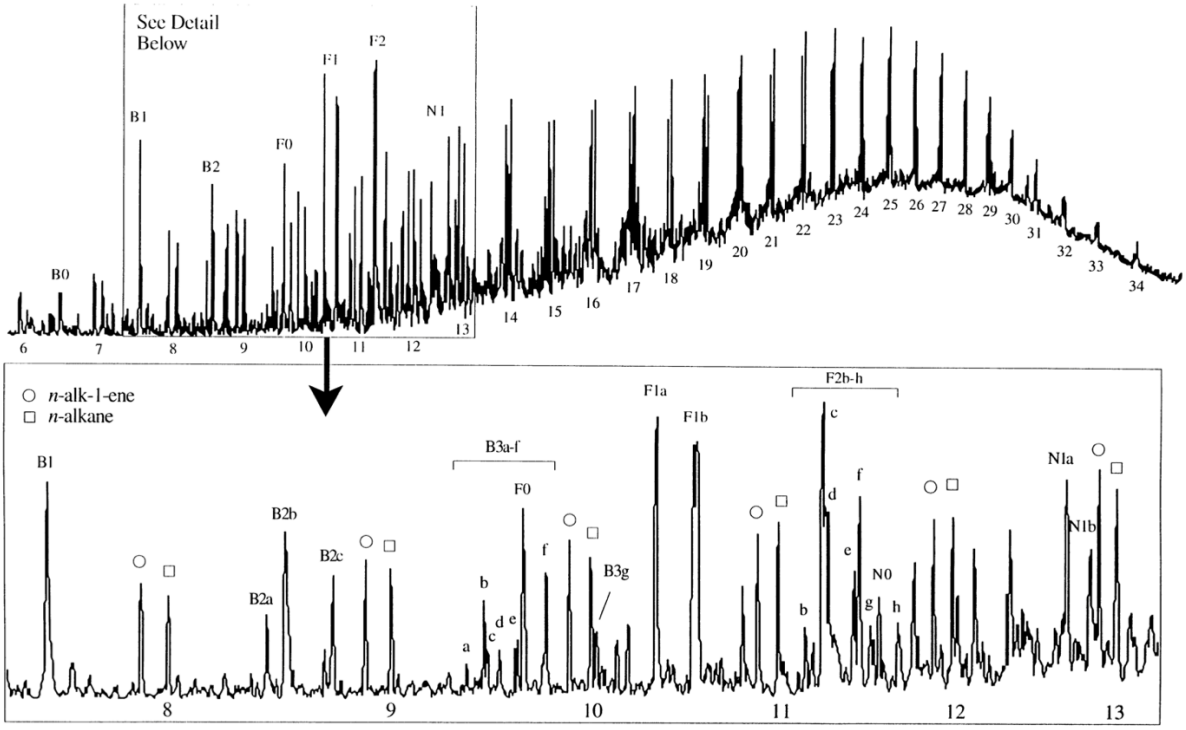

Fig. 4. Total ion current chromatogram (TIC) of the flash pyrolyzates of the Canadian Melville Island cannel coal (sample 15, sporinite-dominated). Part of the chromatogram is enlarged to show detail. Numbers below chromatograms are *n*-alkane carbon numbers. See Table 2 for peak identification.

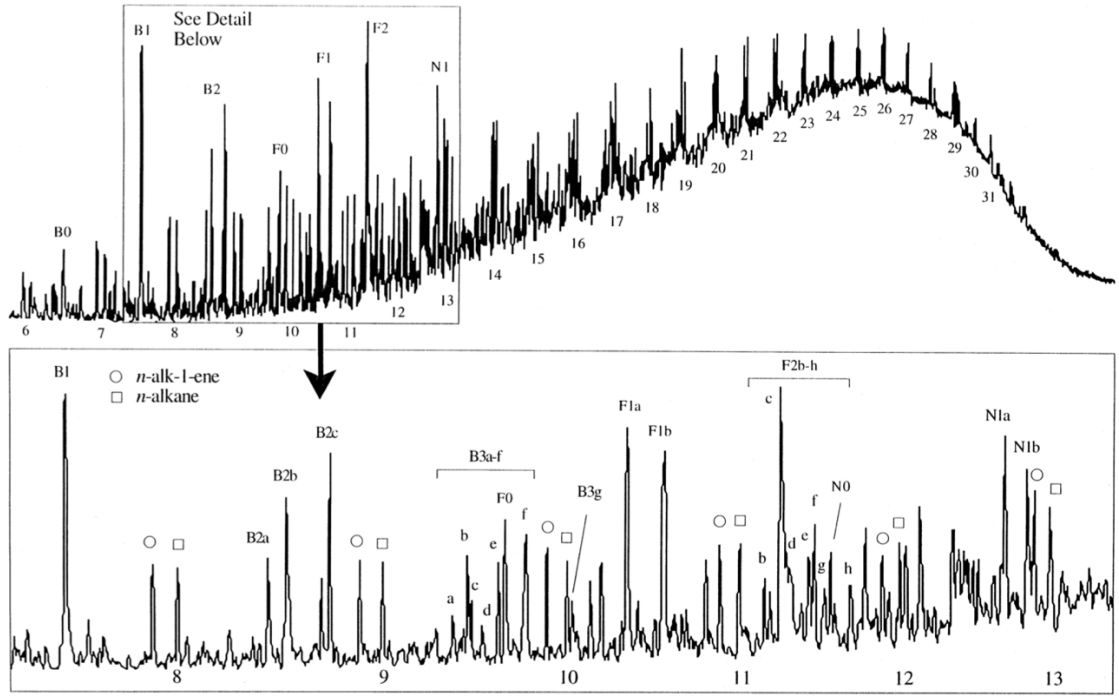

Fig. 5. Dendrogram obtained from an average linkage cluster analysis of data from Py - GC/MS of 14 torbanites and cannel coals. Notice the clear distinction in clustering between the torbanite and cannel coal. Sample 8 (a lamalginite-dominated cannel coal) shows chemical affinity with the torbanites.

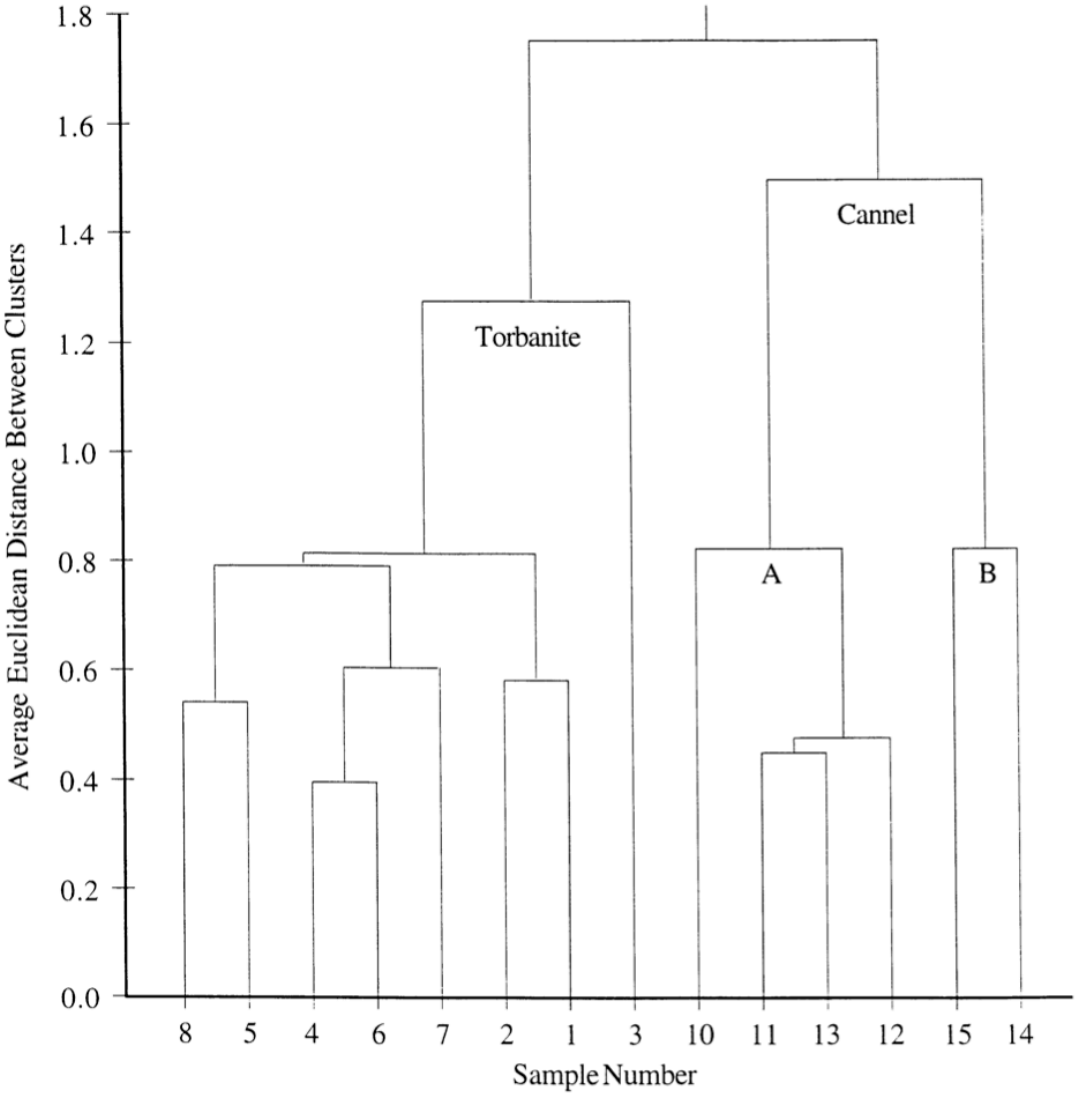

Fig. 6. Relative concentration of the major classes of the pyrolyzates in the 14 torbanites and cannel coals, as a percentage of total peaks quantitated. Refer to the experimental methods section for details of the quantitation procedure. See Table 2 for a complete list of compounds employed, as well as ions used in quantitation. Note that sample 9 was not used in this study.

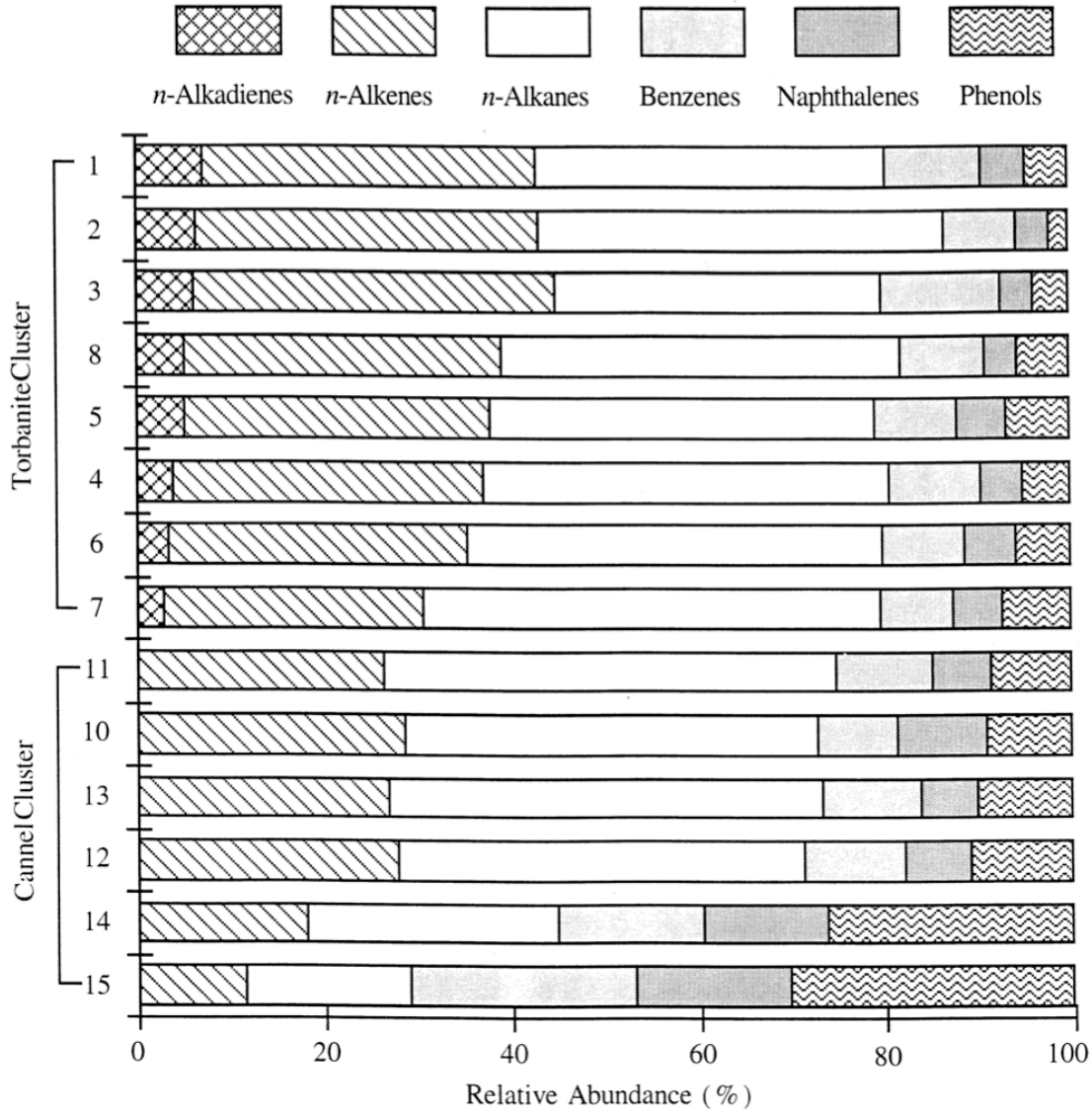

Fig. 7. Relationship between the alginite content and the relative abundance of alkadienes in the pyrolyzates of torbanite (correlation coefficient = 0.91).

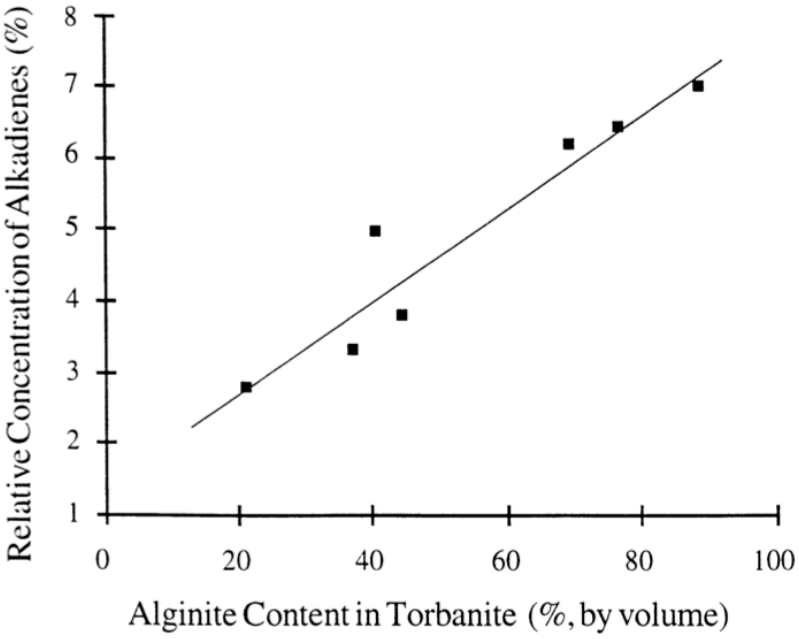

Fig. 8. Straight chain hydrocarbon distributions based on the area summation of C_8-C_{33} *n*-alkadienes, *n*-alkenes and *n*-alkanes of a) the torbanite cluster and b) cannel sub-cluster A. The line is the average distribution of each cluster, the bars are the means, minus and plus one standard deviation. See Fig. 5 for definition of clusters.

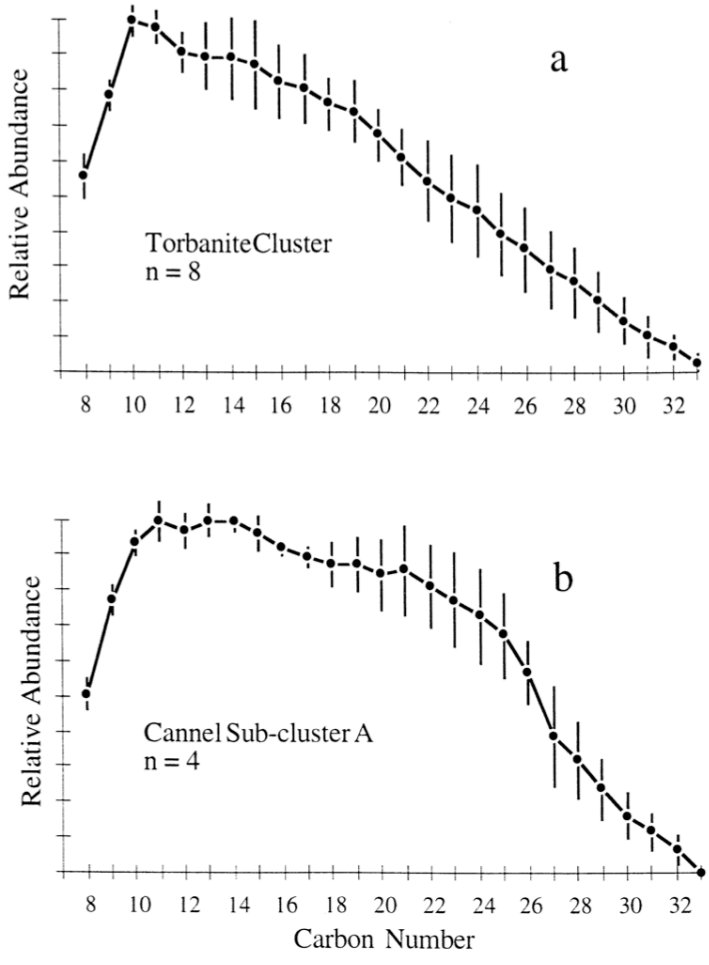

Fig. 9. Summed mass chromatograms of *m/z* 91+ 105+120 illustrating the distribution of C_3-alkylbenzenes in the pyrolyzates of torbanite samples 6 and cannel sample 14. See Table 2 for peak identification.

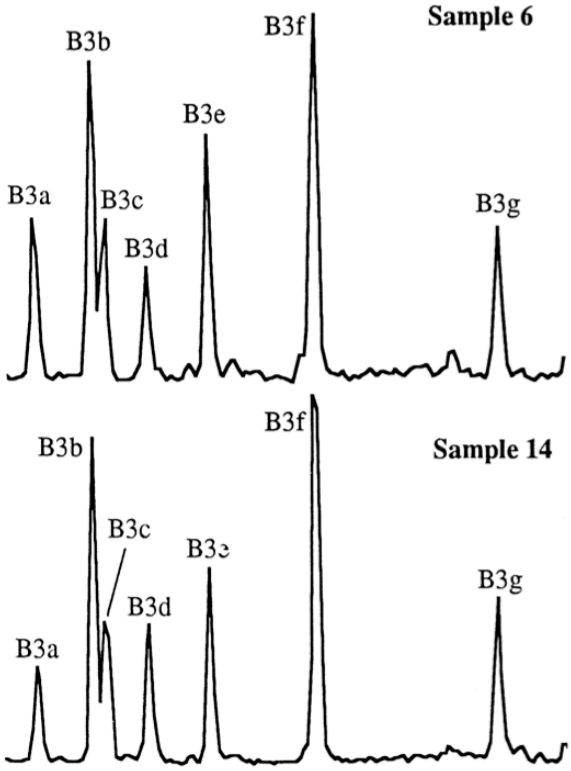

Fig. 10. Summed mass chromatograms of *m/z* 141+156 illustrating the distribution of C_2-alkylnaphthalenes in the pyrolyzates of torbanite samples 6 and cannel sample 14. See Table 2 for peak identification.